EUROFUSION WPBB-CP(16) 15530

A. Tassone et al.

CFD simulation of the magnetohydrodynamic flow inside the WCLL breeding blanket module

Preprint of Paper to be submitted for publication in Proceedings of 29th Symposium on Fusion Technology (SOFT 2016)

This work has been carried out within the framework of the EUROfusion Consortium and has received funding from the Euratom research and training programme 2014-2018 under grant agreement No 633053. The views and opinions expressed herein do not necessarily reflect those of the European Commission.

This document is intended for publication in the open literature. It is made available on the clear understanding that it may not be further circulated and extracts or references may not be published prior to publication of the original when applicable, or without the consent of the Publications Officer, EUROfusion Programme Management Unit, Culham Science Centre, Abingdon, Oxon, OX14 3DB, UK or e-mail Publications.Officer@euro-fusion.org

Enquiries about Copyright and reproduction should be addressed to the Publications Officer, EUROfusion Programme Management Unit, Culham Science Centre, Abingdon, Oxon, OX14 3DB, UK or e-mail Publications.Officer@euro-fusion.org

The contents of this preprint and all other EUROfusion Preprints, Reports and Conference Papers are available to view online free at http://www.euro-fusionscipub.org. This site has full search facilities and e-mail alert options. In the JET specific papers the diagrams contained within the PDFs on this site are hyperlinked

CFD simulation of the magnetohydrodynamic flow inside the WCLL breeding blanket module

Alessandro Tassone[a]*, Gianfranco Caruso[a], Alessandro Del Nevo[b], Ivan Di Piazza[b]

[a] *DIAEE Nuclear Section - Sapienza University of Rome, Corso Vittorio Emanuele II, 244, 00186, Roma, Italy*

[b] *ENEA CR Brasimone, 40032, Camugnano (BO), Italy*

Abstract

The interaction between the molten metal and the plasma-containing magnetic field in the breeding blanket causes the onset of a magnetohydrodynamic (MHD) flow. In order to properly design the blanket, it is important to quantify how and how much the flow features are modified compared with an ordinary hydrodynamic flow. This paper aims to characterize the evolution of the fluid inside one of the proposed concepts for DEMO, the Water-Cooled Lithium Lead (WCLL), focusing on the central cell of the equatorial outboard module. A preliminary validation was required in order to gauge the capability of ANSYS CFX to deal with MHD problems. The buoyant and pressure-driven fully developed laminar flows in a square duct were selected as benchmarks. Numerical results were compared with theoretical solutions and an excellent agreement was found. The channel analysis was realized on a simplified version of the latest available design geometry, developed by ENEA. The simulation highlighted various interesting features, including high velocity jets close to the baffle plate and the onset of an anti-symmetrical electric potential distribution. The electromagnetic pressure drops in the channel were also estimated and found consistent with previous results obtained for similar configurations.

Keywords: MHD, magnetohydrodynamic flow, CFD, breeding blanket, DEMO fusion reactor

1. Introduction

The Breeding Blanket Project (WPBB) was constituted in the 2014 to develop conceptual designs able to satisfy the condition of tritium self-sufficiency for the prototype DEMO reactor. The most promising concept would then be selected in 2020 as the main candidate for the implementation in the demonstrative fusion power plant. The Water-Cooled Lithium Lead (WCLL) is one of the four blankets actually under investigation and the only one to employ water as coolant for both the breeder zone and the first wall. An updated design with modular geometry and a revised layout of the coolant hydraulic circuit was released in the 2015 by ENEA [1][2].

The issues to be addressed by the project are numerous. One of the most compelling is the interaction between the lithium-lead (LiPb) and the magnetic field employed for the plasma containment. This phenomenon modifies the features of the fluid flow, therefore called magnetohydrodynamic. Lorentz forces arise in the bulk of the fluid, obstructing its movement, and cause huge increments in the breeder pressure drops. Moreover, the velocity distribution undergoes drastically alterations; jets, slug flow in the core, suppression of turbulent structures, etc. All these effects must be analyzed to ensure the meeting of the DEMO specifications by the WCLL [3].

The purpose of this study was to investigate the features of the MHD flow in the elementary cell of the equatorial outboard module (EOB) of the WCLL and to provide a first estimation of the electromagnetic pressure drops. Despite the effort of the fusion community spent in the development, a code tailored to simulate MHD flows and extensively validated against theoretically solutions and experimental data is still unavailable [4]. For the purpose of this work, a commercial CFD code with an available add-on featuring the MHD governing equations (ANSYS CFX) was employed. A preliminary validation employing benchmark cases was conducted in order to gauge the capabilities of the code.

2. Formulation

The Navier-Stokes equations must be modified to include the interaction between the conductive fluid and the applied magnetic field, in order to correctly represent a MHD flow. In the following, the ϕ formulation of the MHD governing equations would be employed. If the fluid studied is a liquid metal, it would be characterized by a value of the Reynolds magnetic number (R_m) $\ll 1$ and the influence of the induced magnetic field can be neglected [5]. For a steady and incompressible flow the continuity and

*Corresponding author:

Email address: alessandro.tassone@uniroma1.it (Alessandro Tassone[a])

momentum equations can be written as

$$\nabla \cdot \vec{v} = 0 \tag{1}$$

$$(\vec{v} \cdot \nabla)\vec{v} = -\frac{1}{\rho}\nabla p + \nu \nabla^2 \vec{v} + \frac{1}{\rho}\vec{j} \times \vec{B} + \vec{S_m} \tag{2}$$

where the third term on the right side of 2 represents the volumetric Lorentz force and the fourth a generic momentum source, i.e. due to buoyancy forces. The electric current density $\vec{j}$ is obtained by the Ohm's law and the charge conservation equations

$$\vec{j} = -\nabla\phi + \vec{v} \times \vec{B} \tag{3}$$

$$\nabla \cdot \vec{j} = 0 \tag{4}$$

Combining 3 and 4, it is found the Poisson equation

$$\nabla^2 \phi = \nabla \cdot (\vec{v} \times \vec{B}) \tag{5}$$

which, once solved, provides the electric potential ϕ distribution and, through 3, the current density one.

Finally, the energy equation can be written as

$$\rho c_p (\vec{v} \cdot \nabla) T = k \nabla^2 T + Q \tag{6}$$

where the source term Q accounts for the volumetric power generation inside the fluid, i.e. joule heating or nuclear reactions. The set (1)(2)(5)(6) constitutes the MHD governing equations for a steady and incompressible flow.

Two fundamental parameters influence the flow features: the Hartmann number (M) and the wall conductance ratio (c). The Hartmann number is proportional to the ratio between the electromagnetic and the viscous forces, thus representing the deviation from an hydrodynamic flow.

$$M = BL\sqrt{\frac{\sigma}{\mu}} \tag{7}$$

where B is the intensity of the applied magnetic field; σ and μ are the electrical conductivity and dynamic viscosity of the fluid; L is the flow length scale. For a square duct, two different classes of boundary layers form alongside the walls parallel (side walls) and the ones perpendicular (Hartmann walls) to the magnetic field direction. The scale of these is a function of M through the relations $\delta_S = 1/\sqrt{M}$ and $\delta_H = 1/M$.

The wall conductance ratio represents the influence of the duct wall conductivity on the flow velocity field

$$c = \frac{\sigma_w}{\sigma}\frac{t}{L} \tag{8}$$

where σ_w is the electrical conductivity and t the thickness of the wall. A low value of c (insulating walls) leads to an higher resistance for the currents path and, therefore, to lower pressure drops compared with an high c scenario (conductive walls).

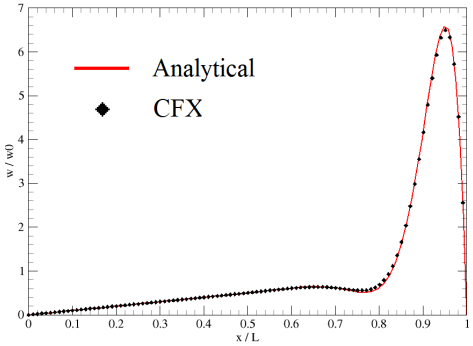

Fig. 1. Buoyant case side wall velocity profile for $M = 4 \cdot 10^2$ and $c = \infty$. The profile was scaled according to [9]

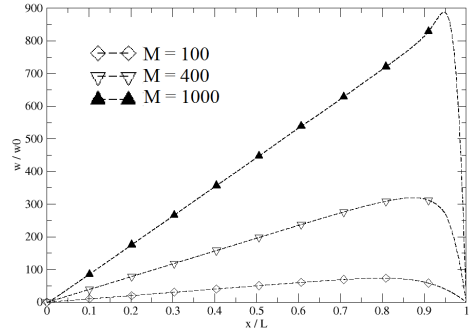

Fig. 2. Buoyant case side wall velocity profile from $M = 10^2$ to 10^3 and $c = 0$. The profile was scaled according to [9]

3. Code validation

Two steady-state fully developed laminar flow benchmarks were employed: a buoyant flow for a pair of differentially heated walls and an adiabatic pressure-driven flow. Analytical solutions ([6], [7] and [8]) and numerical data ([9] and [10]) were used to validate the results. The quality of these was measured with two indexes: a local error (evaluated on the peak velocity value) and an integral error. For the latter, it was considered the non-dimensional flow rate $\tilde{Q}$ ([4]) for the forced convection case, whereas for the buoyant flow benchmark it refers to the integral of the side wall velocity profile. Simulations were conducted with M ranging from 10^2 to 10^4 for insulating and conductive walls. Some selected results are shown in Figure 1, 2 and 3. An overview of the results is available in Table 1.

Table 1
Validation results for peak (p.e.) and integral error (i.e.)

Buoyant test case				P-driven test case			
c	M	p.e.[%]	i.e.[%]	c	M	p.e.[%]	i.e.[%]
0	100	0.68	n.a.	0	500	n.a.	0.54
	400	4.08			5000		0.21
	1000	2.08			10000		0.01
					15000		0.44
∞	100	2.01	0.79	∞	100	2.85	0.03
	400	1.26	1.49		400	3.08	0.14
	1000	2.20	1.46		1000	7.14	0.13

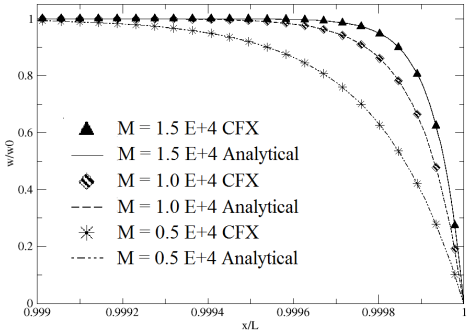

Fig. 3. Pressure driven case Hartmann wall velocity profile from $M = 0.5 \cdot 10^4$ to $1.5 \cdot 10^4$ and $c = \infty$. The profile was scaled with the center duct velocity.

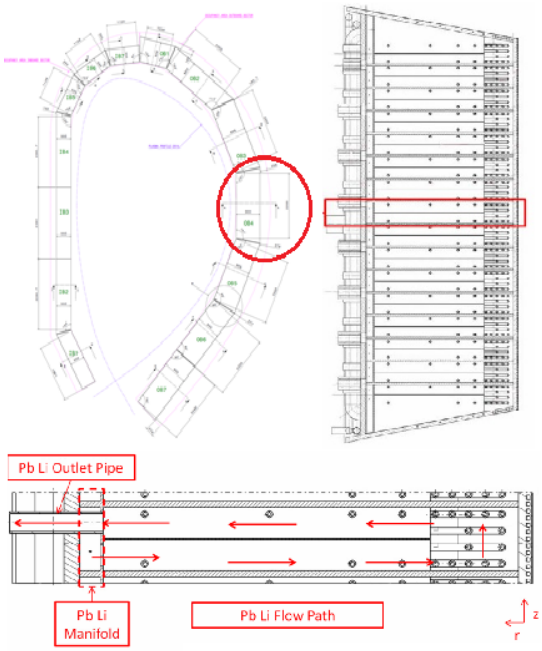

Fig. 4. Position in the blanket segmentation and layout of the EOB module (top); detail of the elementary cell (bottom)[2]

4. WCLL cell analysis

The updated geometry of the WCLL elementary cell (Fig 4) was employed to perform the analysis [2]. The temperature of the LiPb was assumed as constant and equal to the inlet/outlet value (i.e. 599 K). Moreover, the volumetric heating was not modeled and any thermal flux from the LiPb to the channel walls, and vice versa, was neglected. Accordingly, the water pipes were removed from the channel geometry.

The magnetic field was assumed constant with toroidal and poloidal components imposed at their average values, calculated between the first wall and the manifold [1]. Due to this assumption, the 3D MHD effects were simulated only in the bend. In order to improve the convergence

[1] 4 T(toroidal) and 1.175 T [2]

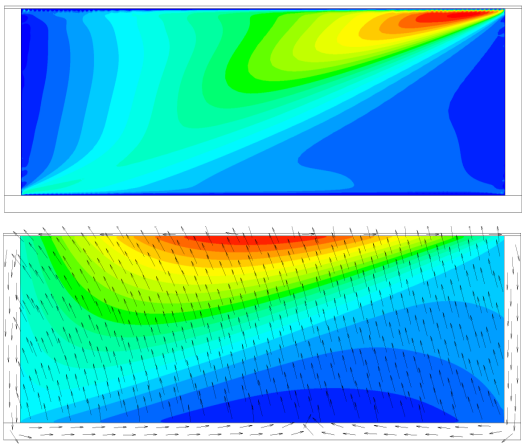

Fig. 5. Velocity (top) and electric potential contour with current paths (bottom) for the inlet duct

velocity and numerical stability of the simulation, two dummy walls were rendered in the bend region to avoid the breeder movements toward the nearby (not-modeled) channels. These were considered as formed by solid LiPb, electrically equivalent to the fluid.

The LiPb enters the cell in the bottom channel (inlet) then flows radially to the bend located near the first wall. Here the fluid rises in the poloidal direction and then bends again radially, leaving the cell through the top channel. At the inlet the flow is assumed to be in fully developed state with an average velocity of 1.55 mm/s. Relevant simulation parameters are available in Table 2.

The reference flow for this simulation is the pressure-driven laminar flow in a rectangular duct with walls of finite conductivity [7]. However, the complex topology of the magnetic field and the different value of the wall conductance ratio assumed by the duct walls drastically change the flow features compared with the reference.

Due to the presence of both toroidal and poloidal components for the magnetic field, the electric potential distribution in the fluid is no longer symmetric across the duct mid-plane. The induced currents modify their paths to maintain themselves perpendicular to the magnetic field lines. The peak of the electric potential therefore shift toward the corners of the duct sited on the direction perpendicular to the magnetic field lines. Close to the other corners a weakening of the electric potential (and therefore of the electromagnetic drag) occurs with the appearing of high velocity jets. The low conductivity ratio of the baffle enhances the jet nearby, whereas the opposite happens for the one close to the stiffener. In Fig. 5 and 6, the electric potential and velocity contour for the cell are shown.

The fully developed state is maintained for the most part of the inlet channel due to the hypothesis made at the inlet and the intensity of the magnetic field. This happens because of the induced currents being confined to the cross-section. When the fluid approaches the bend region, an axial potential difference appears, driven by the velocity

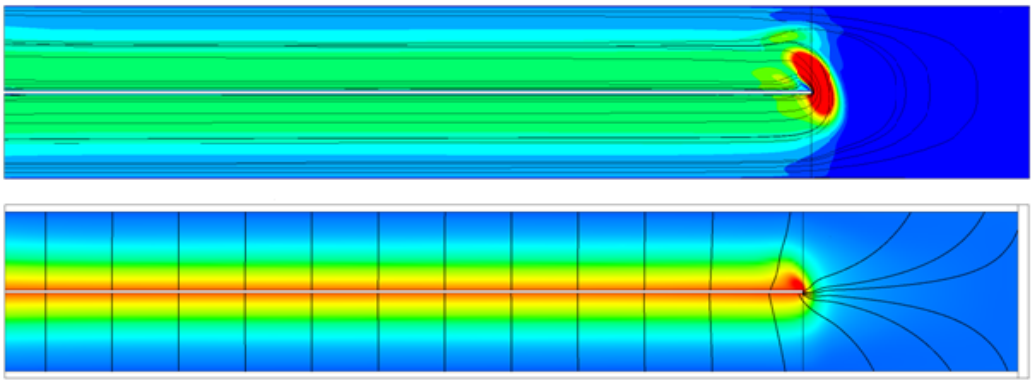

Fig. 6. Velocity (top) and electric potential contour with current paths (bottom) for the whole cell

Table 2
WCLL simulation parameters

Toroidal (L)	Poloidal (H)	Axial (Z)	M	c
117 cm	33.1 cm	800 cm	985	2.5 ÷ 10

gradient between the fluid in the inlet channel and in the bend. Axial currents are induced and the flow becomes 3D. This condition does not persist in the outlet channel where the magnetic field quickly restores the 2D flow.

The overall channel pressure drop amounts to 178.33 Pa (of which only the 3% of the total ascribable to the 3D pressure drops) a value that is comparable with the one calculated by de les Valls et al. [11] for a similar configuration and perfectly conducting walls (248 Pa). The differences between the two values can be explained due to the less conductive walls of the WCLL layout, the weaker magnetic field, more realistic inlet conditions and a larger bend region.

5. Conclusions

This activity investigated the MHD flow of the LiPb inside the central cell of the EOM of the DEMO WCLL blanket concept with the help of a main-purpose CFD code ANSYS CFX. Validation conducted on selected benchmarks demonstrated that the code was suitable for solving MHD problems. A simplified analysis of the WCLL elementary cell was performed. The onset of an asymmetric electric potential distribution was found in the cell with highly velocity jets close to the baffle. The flow maintained the purely 2D state throughout the cell with axial currents and 3D flow being present only in the bend. The MHD pressure drops are calculated as 178.33 Pa.

The simulation results confirm that insulating flow channel inserts (FCI) are not required to decouple the fluid and the duct walls. However, in the real cell the magnetic field gradient and the coolant pipes would extend the presence of the 3D regime to the whole cell causing higher MHD pressure drops. A study with more realistic assumptions would be conducted in the future, extending the analysis to the manifold region.

Acknowledgements

This work has been carried out within the framework of the EUROfusion Consortium and has received funding from the Euratom research and training programme 2014-2018 under grant agreement No 633053. The views and opinions expressed herein do not necessarily reflect those of the European Commission.

References

[1] L. Boccaccini, et al., Objectives and status of eurofusion demo blanket studies, Fusion Engineering and Design (2016).

[2] A. Del Nevo, et al., Wcll design report on cad, neutronics, thermo-hidraulycs and thermo-mechanical analyses, WPBB-DEL- BB- 3.2.1-T002-D001 (2016).

[3] S. Smolentsev, et al., Mhd thermofluid issues of liquid-metal blankets: phenomena and advances, Fusion Engineering and Design 85 (2010) 1196–1205.

[4] S. Smolentsev, et al., An approach to verification and validation of mhd codes for fusion applications, Fusion Engineering and Design 100 (2015) 65–72.

[5] P. A. Davidson, An introduction to magnetohydrodynamics, volume 25, Cambridge university press, 2001.

[6] L. Bühler, Laminar buoyant magnetohydrodynamic flow in vertical rectangular ducts, Physics of Fluids (1994-present) 10 (1998) 223–236.

[7] J. Hunt, Magnetohydrodynamic flow in rectangular ducts, Journal of Fluid Mechanics 21 (1965) 577–590.

[8] J. Shercliff, Steady motion of conducting fluids in pipes under transverse magnetic fields, in: Mathematical Proceedings of the Cambridge Philosophical Society, volume 49, Cambridge University Press, 1953, pp. 136–144.

[9] I. Di Piazza, L. Bühler, A general computational approach for magnetohydrodynamic flows using the cfx code: buoyant flow through a vertical square channel, Fusion Science and Technology 38 (2000) 180–189.

[10] C. Mistrangelo, L. Bühler, Numerical study of fundamental magnetoconvection phenomena in electrically conducting ducts, IEEE Transactions on Plasma Science 40 (2012) 584–589.

[11] E. M. de Les Valls, et al., Modelling of integrated effect of volumetric heating and magnetic field on tritium transport in a u-bend flow as applied to hcll blanket concept, Fusion Engineering and Design 86 (2011) 341–356.